



*The Society for engineering
in agricultural, food, and
biological systems*

Paper Number: AA05-001
An ASAE Meeting Presentation

AERIAL SPRAY PLUME DISPERSION MEASURED WITH LIDAR

David R. Miller

University of Connecticut, Natural Resources Management and Engineering Department, Storrs,
CT 06269-4087.

April L. Hiscox

University of Connecticut, Natural Resources Management and Engineering Department, Storrs,
CT 06269-4087

Carmen J. Nappo

NOAA, Atmospheric Turbulence and Diffusion Division, Oak Ridge TN

James Ross

New Mexico State University, Entomology, Plant Pathology and Weed Science
Department, Las Cruces, NM 88005

**Written for presentation at the
2005 ASABE/NAAA Technical Session
Sponsored by ASABE Technical Committee PM23/6/2
39th Annual National Agricultural Aviation Association Convention
Silver Legacy Hotel and Casino, Reno, NV
December 5, 2005**

The authors are solely responsible for the content of this technical presentation. The technical presentation does not necessarily reflect the official position of the American Society of Agricultural Engineers (ASAE), and its printing and distribution does not constitute an endorsement of views which may be expressed. Technical presentations are not subject to the formal peer review process by ASAE editorial committees; therefore, they are not to be presented as refereed publications. Citation of this work should state that it is from an ASAE meeting paper EXAMPLE: Author's Last Name, Initials. 2003. Title of Presentation. ASAE Paper No. AA03-00x. St. Joseph, Mich.: ASAE. For information about securing permission to reprint or reproduce a technical presentation, please contact ASAE at hq@asae.org or 269-429-0300 (2950 Niles Road, St. Joseph, MI 49085-9659 USA).

Abstract. A field study of aerial spray movement and dispersion was conducted at the New Mexico State University spray study site on the USDA Jornada Desert research ranch in April 2005. The purpose of the study was to measure the plume movement dynamics and deposition of fine droplet applications during calm, stable conditions. Spray plume movement and dispersion was measured and recorded with a portable elastic-backscatter LIDAR. Supporting meteorology, air turbulence and micro-movements were made simultaneously with sonic anemometers. The amount of spray material remaining in the air decreased rapidly for the first minute, and thereafter remained constant and drifted as a definable plume with the slight air drainage currents. The paper presents LIDAR generated graphics demonstrating the plume movement and dispersion.

Keywords. Vector Control, Spray Drift, Plume, Dispersion, LIDAR, Aerial Application, Meteorology.

INTRODUCTION

Applications of mosquito adulticides by air are most effective when the spray reaches the target area, remains airborne and spreads significant distances near the ground in the target area. This requires spraying small droplets which will remain suspended, during meteorological conditions which will suppress the upward dispersion of the spray and move the spray cloud across the target area near the ground and vegetation. On the other hand, control of crop pests and weeds by aerial applications of chemical or biological pesticides, require exactly the opposite conditions. That is, large droplets which will fall out of the air and meteorological conditions which spread and disperse the material on the ground and vegetation in predictable swaths with minimum drift. In either case, the applicator is responsible for knowing the amount of material present at any given time and location after an application. To date, spray concentrations drifting in the air can only be estimated by models such as AgDrift (Bird et al., 2002), or by interpreting dosages accumulated in point samplers downwind of a spray operation (Miller et al. 2000).

This paper reports on a study to remotely measure the material remaining airborne and the spread of plumes from vector control type aerial applications.

METHODS

General Approach

The field study of aerial spray movement and dispersion was conducted at the New Mexico State University spray study site on the USDA Jornada Desert research ranch (Lat. 32.31N, Long. 106.75W) in April 2005. The site was flat with low, ~1-2 m tall, sparse desert vegetation with unobstructed fetch in all directions for at least 10 km.

The New Mexico State University Cessna T188C equipped with Micronair AU5000 rotary atomizers applied oil based tracer at a rate of 21.6 gallons per acre. Average VMDs were 37.3 μ for three replications from the Micronair AU5000 simulating the aircraft application in the wind tunnel. DV0.1 was 13.3 μ m and DV 0.9 was 82.8 μ m. Five single-swath passes were conducted near dawn on April 27, 2005 at times in Table 1. Sunrise was at 6:30 MDT.

Table 1. Meteorological Conditions at the Spray Height During Single Spray Passes (5 minute average)

	Pass 1	Pass 2	Pass 3	Pass 4	Pass 5
Time (MDT)	6:17:47	6:24:51	6:50:54	6:56:59	7:04:09
U (m/s)	1.44	0.83	1.99	1.63	2.21
U _{dir} (degrees)	32	46	71	60	58
z/L	126.5	36.0	20.5	185.8	-28.53
T	8.5	8.9	9.2	9.4	9.7
RH	74	74	57	52	49

Cross-sections of the spray plumes were scanned from ~500 m away (to the West) with the University of Connecticut portable elastic-backscatter LIDAR (Figures 1 and 2). Cross-sectional scans through the plumes measured movement and dispersion every 2.4 seconds for 5 to 10 minutes after the airplane pass. After this length of time the residual plume generally drifted out of the lidar scan angles. Five single-pass spray applications were made. Supporting meteorology and air turbulence and air-movements were made simultaneously with sonic anemometers on an 11 m tower located ~ 50 m from the spray swath.



Figure 1. Spray plane pass, 600 m to the East of the lidar position.



Figure 2. UCONN Scanning, Elastic-Backscatter LIDAR

The amount of spray material remaining in the plume over time was determined from the initial drop size distribution and the application rate. Droplet deposition and shrinkage due to evaporation was calculated and subtracted from the initial total to arrive at the remaining material still suspended in the air. Then the lidar backscatter/mass ratio was used as the calibration for the lidar. Initial size distributions from the Micronair sprayers were measured in the NMSU wind tunnel with a Malvern Inc. Drop sizer.

Drop size distribution

The initial drop size distribution for the aircraft and Micronair setup and operation was used as the initial estimation of the amount of material still in the air at a time, t , after release. For this experiment it was desired to keep the drops in the air for the longest amount of time, so a very high atomization rate was used (VMD=37.1 μm , DV_{0.1}=13.5 μm , DV_{0.9}=82.7 μm). For all of the following calculations thirty drop size classifications between 0.371 μm and 196.21 μm were used. These drops sizes are representative of spray used in vector control rather than crop application. A simplified model of how this distribution would change over time was used following the techniques of Flesch and Aylor, 2000. A hard-core model was assumed, meaning that an individual droplet can be modeled as an oil droplet surrounded by water. The diameter of the oil center can be estimated as:

$$D_f = D_0 f_{p0}^{1/3}$$

Where, D_0 is the initial droplet diameter, and f_{p0} is the volume fraction of the nonvolatile pesticide in water (Flesch and Aylor, 2000), in this case the nonvolatile portion was 10% oil. Volatilization at the theoretical water evaporation rate was assumed with no further evaporation once the droplet reached its oil core, after the experimental results of Luo et al. (1994). So D_f represents the final droplet diameter. Evaporation was modeled as:

$$\frac{dD}{dt} = \frac{4\eta m_w}{\rho_w R D_0} \left(\frac{e_w}{T_a} - \frac{e_{sw}}{T_a} \right)$$

after Baron and Willeke (2001), where η is the atmospheric diffusivity, m_w is the molecular weight of water, ρ_w is the density of water, R is the gas constant (8.3144 m³kPa/kmol K), e_w is the vapor pressure of water, e_{sw} is the saturation vapor pressure of water and T_a is the air temperature.

After shrinking through evaporation, the settling velocity of the drop was found from:

$$v_s = 4.47e - 3D - 0.191 \quad D > 100 \mu m$$

$$v_s = 3.2e - 5D^2 - 6.4e - 8D^3 \quad D < 100 \mu m$$

where, D is the droplet diameter in μm , and the settling velocity, v_s is in m/s (Flesch and Aylor, 2000). For any given time, t , if the droplet had theoretically fallen a distance greater than the release height (11.9 meters), it was removed from subsequent distributions.

To determine the volume fraction for each size class, it was assumed that the number of particles of each size remained the same, unless they had fallen to the ground, in which case the number was replaced by zero. This assumption does not account for particle growth through coagulation or nucleation, but these processes are likely to produce little error in active ingredient accounting since they occur mostly with very small aerosols which, even when aggregated, won't fall out. By changing the particle diameters and number of particles through evaporation and settling as described above, it is possible to calculate new mass distributions over time and therefore new volume fractions to find a final particle size distribution, and a total mass still aloft for any later time. This yields a predicted mass aloft of:

$$M(t) = \sum_i N_i M_i(t)$$

where, i represents each size classification, N is the number of particles and

$$M_i(t) = \rho_{H_2O} \frac{\pi}{6} [D_i(t)^3 - D_{if}^3] + \rho_{oil} \frac{\pi D_{if}^3}{6}$$

Figure 3 shows the results of this calculation to find downwind drop size distributions for up to 420 seconds (7 minutes) after the release time. The calculated particle size distributions for one minute intervals can be seen and the sharp drop offs are due to the assumption that all of the droplets larger than a particular size drop out.

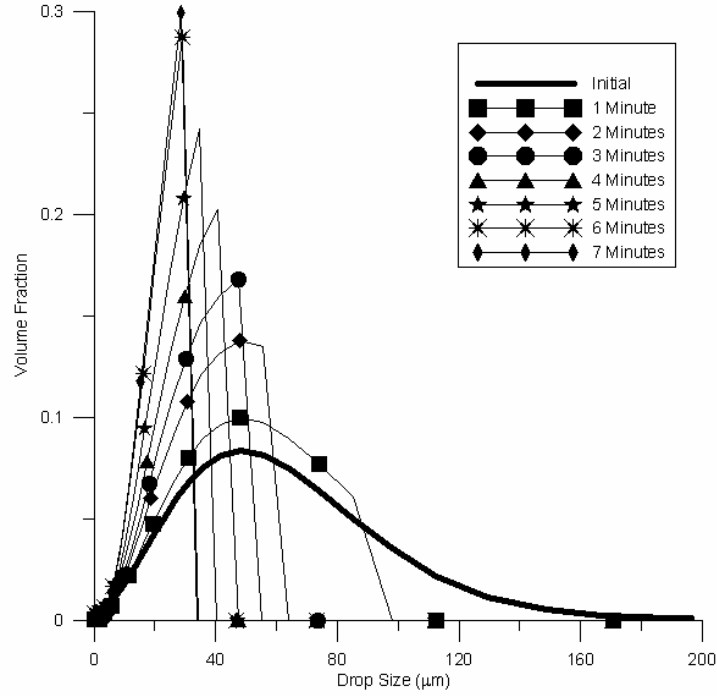


Figure 3: particle size distributions over time

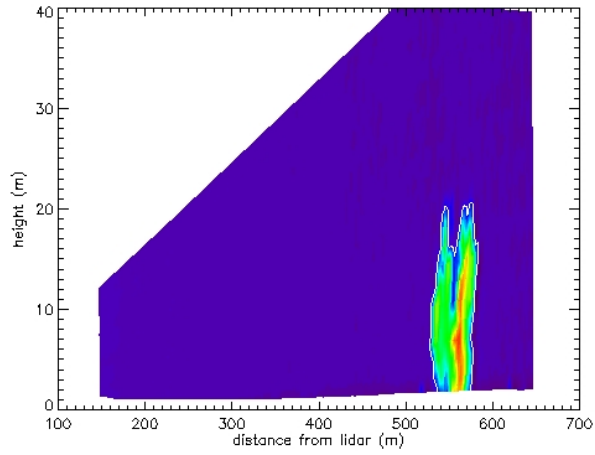
Relation to Lidar data

Using plume identification methods similar to Hiscox et al., 2004, the area, horizontal movement and total backscatter for each cross-sectional slice of the lidar was calculated by defining a single backscatter level to be the edge of the plume. An example plume and its statistics can be seen in figure 4.

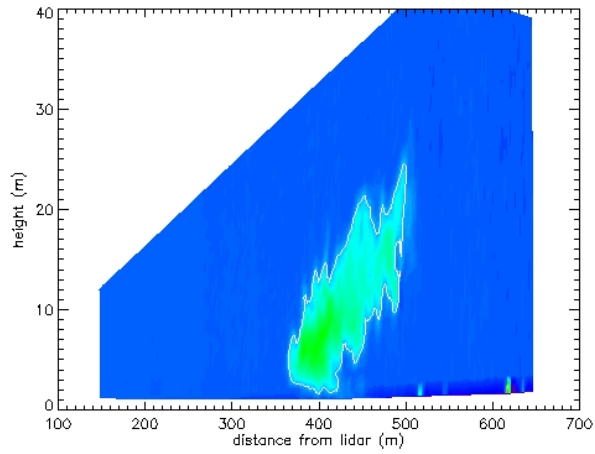
To explore the relationship between lidar backscatter and mass, the predicted mass aloft was converted to a concentration value by dividing by the volume of the first usable plume cross-section, $Q_p(t) = M(t)/V_0$, where V_0 was 107.6 m^3 , the volume of the first full slice of the spray plume. The concentration values were compared with the total lidar backscatter per unit area across the plume at 30 second intervals for the 3 usable minutes of pass 1 (Figure 5). The slope of the linear relationship was then used as a conversion factor, α , to estimate the concentration remaining in the air.

$$Q_{lidar}(t) = \frac{\beta_{lidar}(t)}{V_t} * \alpha$$

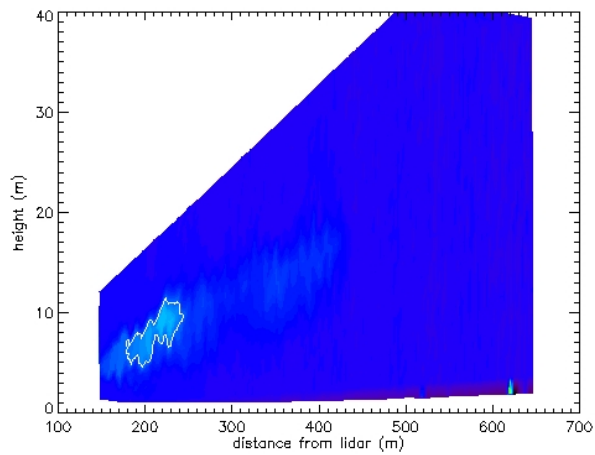
where $\beta_{lidar}(t)$ is the total backscatter in the identified plume and V_t is the volume of the plume at time t after release. The volume of each slice is taken to be the area identified by the edge of the plume multiplied by the lidar beam width at 600m. In actuality, the lidar beam width increases with distance from the lidar, no corrections for this were made in these calculations. The effects of this assumption will be addressed in future study. All of the lidar values were then adjusted to convert their values to mass, a plot of the results is shown in figure 7.



(a)



(b)



(c)

Figure 4: Lidar slices at 45.1 seconds (a), 180.4 seconds (b), and 361.2 seconds (c) after the release of the plume. Plume cross sectional areas are 766.33 m^2 , 1320.7 m^2 , and 174.8 m^2 respectively.

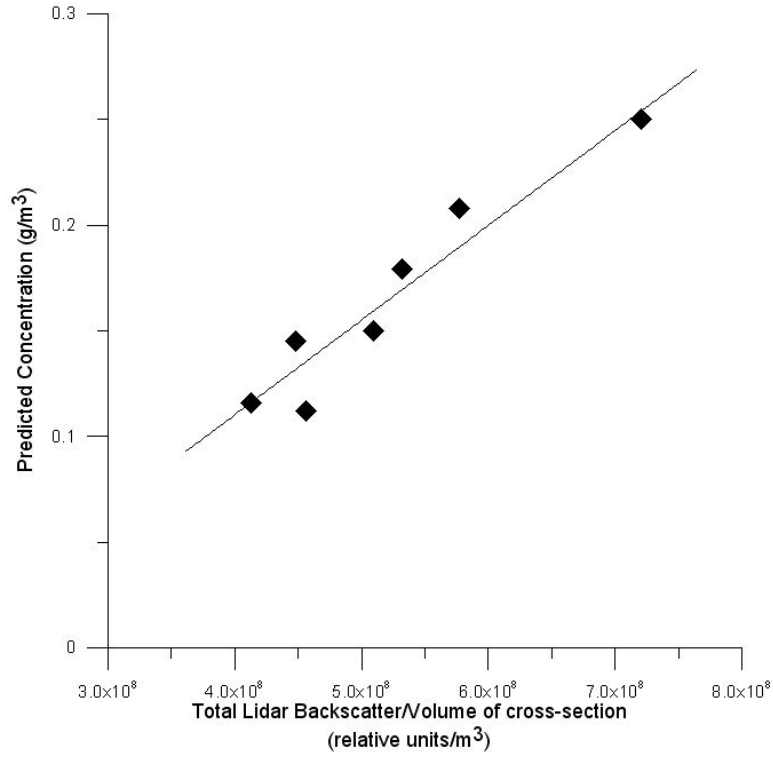


Figure 5: Predicted concentration aloft vs. total lidar backscatter per unit volume. Total lidar backscatter per unit volume values are for 30 second intervals after the plume release time. The slope of the linear fit shown on the graph is $\alpha = 3.7e-13$.

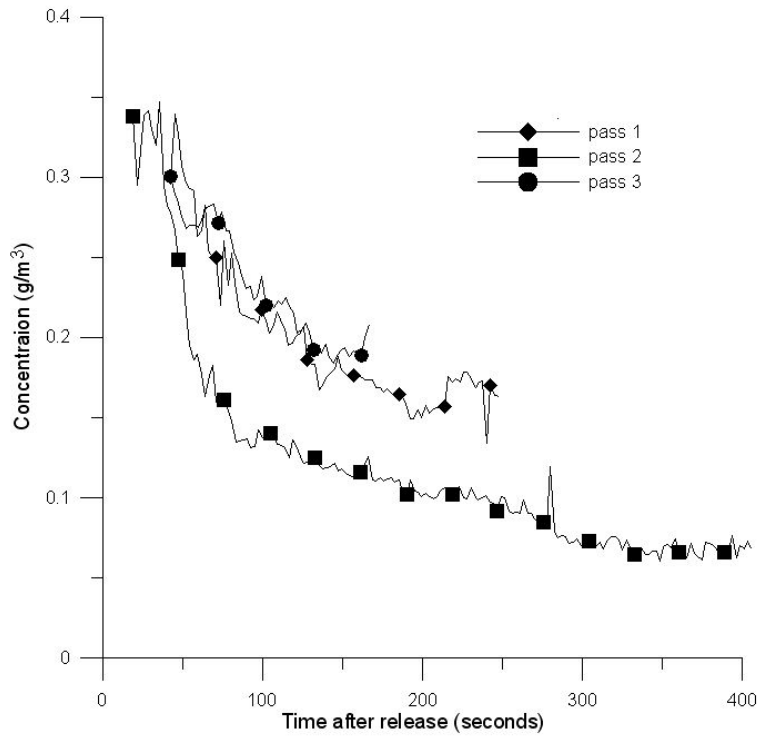


Figure 6: Total lidar backscatter per unit volume converted to units of mass concentration.

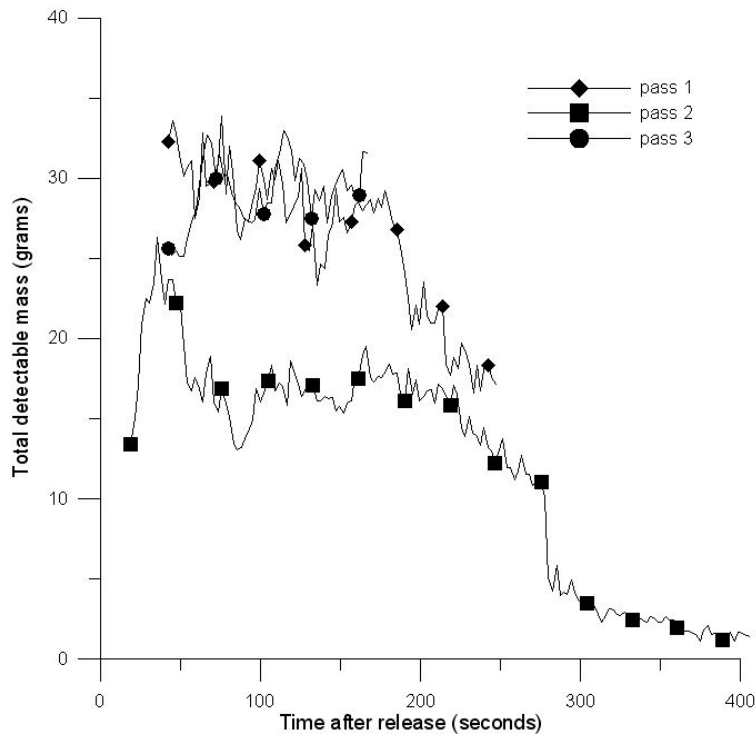


Figure 7: Total mass remaining in the air

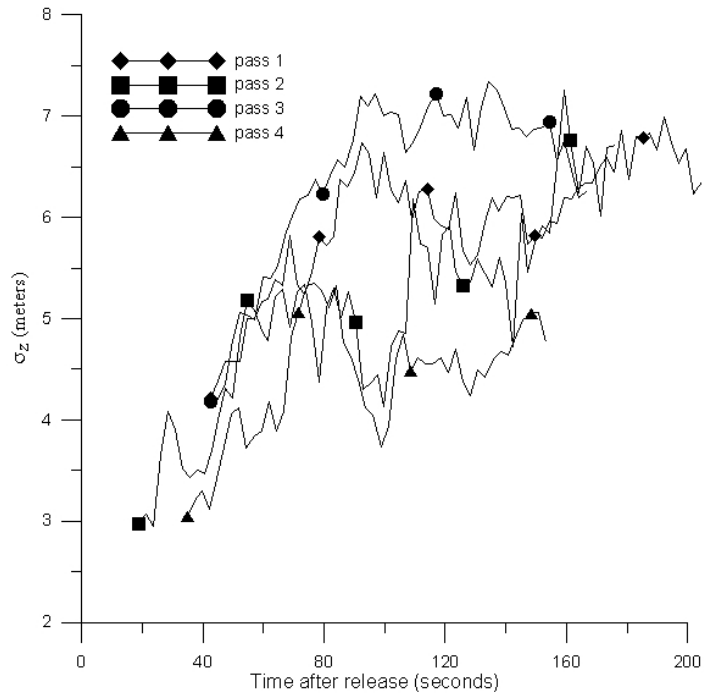
RESULTS

Effect of atmospheric stability on plume spread.

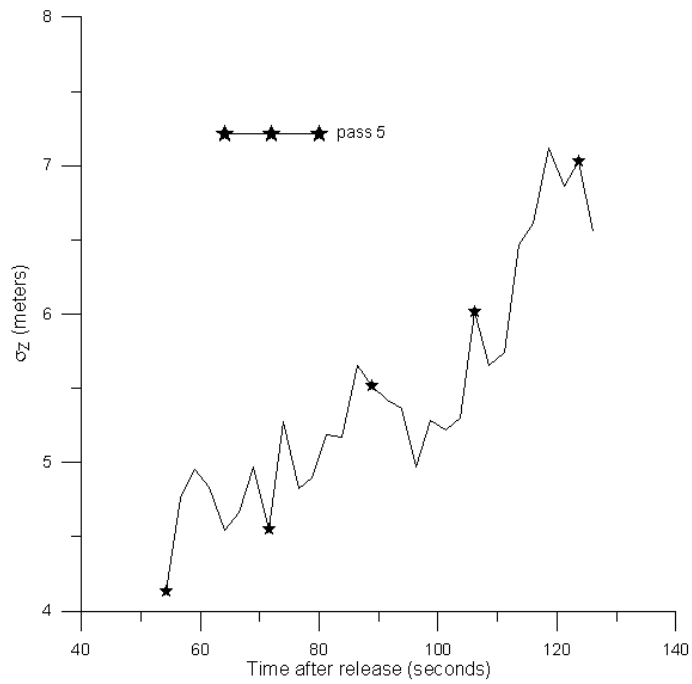
The dispersion (vertical spread) rate of the suspended plumes were quantified with the lidar. Standard deviations of the across plume concentrations (called the dispersion parameters) were determined from the lidar returns from each cross-sectional slice using the methods of Hiscox et. al. (2004).

Local sunrise, when the sun cleared the mountains to the East, was about 25 minutes after the solar time sunrise at 6:30 MDT. This occurred between runs 4 and 5 and rapidly changed the conditions from stable to unstable. Figure 8 displays the dispersion parameters for three minutes after each spray run and demonstrates the effect of local atmospheric stability on the vertical plume spread. Figure 8a shows the dispersion parameters increasing (i.e. the plume expanding) during stable conditions for about 2 minutes after the airplane pass. After that the dispersion parameter remained relatively constant (the plume stopped expanding). On the other hand, during unstable conditions, shown in figure 8b, the plume continued expanding at a relatively regular rate for the entire period.

In figure 8a, the initial expansion was due to the turbulence caused by the aircraft passing and it took about 100 sec before the disturbance dissipated enough for the stable, non-turbulent, atmospheric conditions to suppress the vertical spread of the plume. In figure 8b, the initial expansion rate was continued, likely indefinitely, because the air was unstable and turbulent.



(a) Stable conditions



(b) Unstable conditions

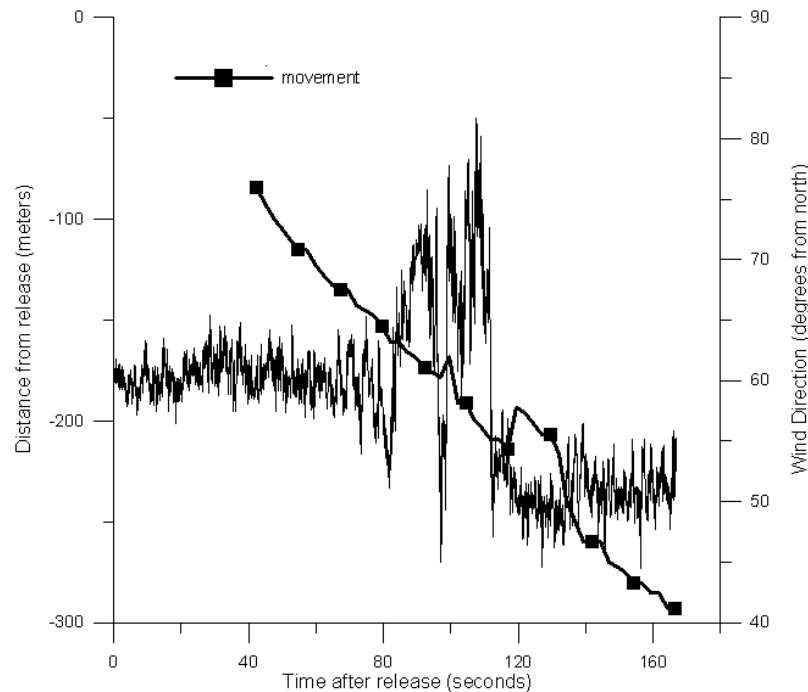
Figure 8: Vertical plume dispersion in stable and unstable conditions.

Amount of spray material remaining suspended in the air.

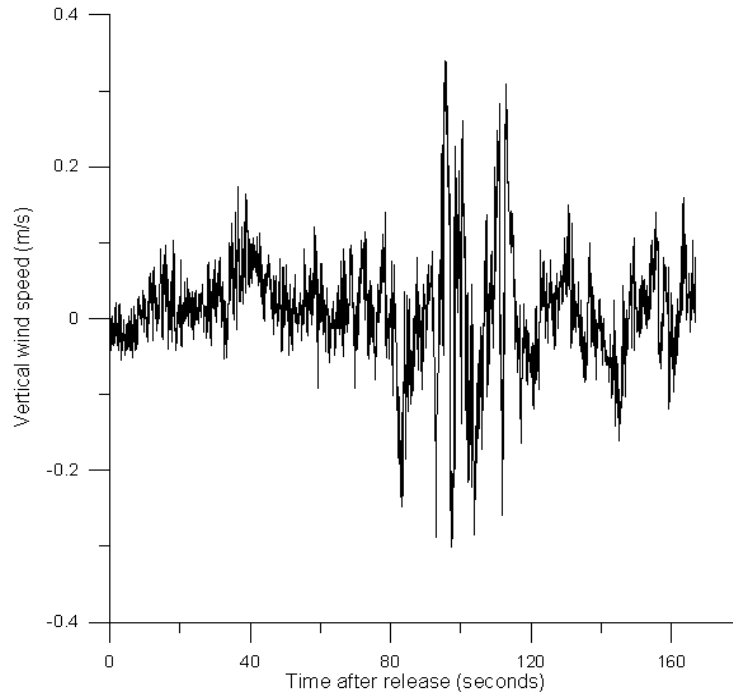
Figure 7 shows the concentrations of spray material remaining in the air decreased rapidly for the first minute, when all the large ($> 40 \mu$) droplets were falling out and the plume was expanding. After that the amount of material suspended decreased less rapidly as evaporation alone continued decreasing the total mass in the air.

Plume meander.

Whole plumes move back and forth and up and down due to large scale motion changing the wind direction slowly. In this case the wind direction was quite stable throughout the hour and no large scale meander was measured. But periodic atmospheric waves moved across the site at a frequency of about every 10 minutes. These wave motions interrupted the plume movement for periods of 30 to 120 seconds. Although the waves moved the plume for distances of up to 200 m, they had little detectible effect on the plume concentrations or spread. Figure 9 demonstrates one of these wave events and its effect on pass 3. Graph a shows the wind direction time series during the period the plume was being monitored by the lidar with the plume center location in relation to the release point overlaid. A wave event passed through at 80 seconds after the release, moving the wind direction ~ 20 degrees to the right. The regular movement of the plume was interrupted by the wave moving through and moved the plume about 25 meters back and then forward until the plume was moving at its previous rate and location. Graph b is the vertical component of the wind during this period and it shows a large up and down motion while the wave is passing.



(a)



(b)

Figure 9: (a) Plume movement towards the lidar and wind direction for pass 3. (b) vertical component of the wind speed for pass 3.

CONCLUSION

Micronair atomizers produced small droplets resulting in drifting plumes which contained about 40% of the active ingredient and 10% of the total mass sprayed after several minutes. Concentrations after two minutes were on the order of 0.1 g/m^3 . In stable conditions the plumes expanded radially for about 1.5 minutes under the influence of the wing tip vortex turbulence. Then the stable atmosphere suppressed any further vertical dispersion. The plume in unstable conditions continued expanding indefinitely. The plumes meandered very little during the first few minutes after spraying. Short time scale, atmospheric wave motions had little effect on the plume dispersion or movement directions.

ACKNOWLEDGEMENTS

This research was supported by the US Army Research Laboratory, New Mexico State University, and the Storrs Agricultural Experiment Station.

REFERENCES

- Baron, P.A. and K. Willeke, "Aerosol measurement: Principles, techniques and applications", Wiley-Interscience, 2001.
- Flesch, T.K and D.E. Aylor, "A lagrangian stochastic dispersion model for assessing pesticide spray drift in an orchard canopy", USEPA Technical Report, April 2000.
- Hiscox, A.L., D.R. Miller, and C. Nappo, "Plume model parameters measured with Lidar", ASAE paper no. 051144, annual meeting 2005.
- Miller, D. R., T. E. Stoughton, W. E. Stienke, E. W. Huddleston and J. B. Ross. 2000. Atmospheric Stability effects on pesticide drift from an orchard sprayer. *Trans ASAE* 43(5):1057-1066.
- Luo, Y., D. R. Miller, X. Yang, M. A. McManus and H. M. Krider. 1994. Characteristics of Evaporation From Water Based Bacterial Pesticide Droplets. *Trans. ASAE* 37(5):1473-1479.